EFFECT OF HARMONICS ON A SOLID-ROTOR INDUCTION MOTOR

Asst. Prof. Dr. Ali M. Saleh **Ahmed Th. Radhi**
College of Engineering University of Baghdad

ABSTRACT
The paper records a study of an investigating the performance of a solid-rotor induction motor with a rectilinear inverter excitation to identify the effects of the associated time harmonics. The performance is determined experimentally by using a stator of a three-phase laboratory induction motor that is fitted with a solid-steel rotor and compared with the theoretical model developed which uses the Fourier components of the supply voltage waveform. Final conclusions are drawn from comparing motor performances with sinusoidal and inverter excitations. An equivalent circuit model is developed to determine the harmonic currents. The development of the theoretical model make use of the results of existing field analyses. Harmonic currents and other performance details including the possible interactions between the co-existing harmonics are determined and discussed. The measured values of torque, input current and power over full speed range with the two types of excitation are presented, and compared with the theoretical values. The waveforms of current, phase and line voltages are analyzed experimentally and compared with simulation results. The theoretical results correlate well with measured results and the significant harmonic effects are identified.

الخلاصة

: تسجل هذه الأطروحة دراسة لبحث أداء المحرك الحثي من النوع ذو الدوار الصلب (Solid-Rotor) بتغذيته من خلال فولتية العاكس للتعرف على التأثير المرافق للتوافقيات الموجودة ضمن فولتية العاكس. لقد تم استنتاج الأداء عمليا باستخدام محرك حثي الجزء الثابت له يعمل مع دوار من نوع الصلب وقورن مع النموذج النظري الذي تم باستخدام مركبات فورير (Fourier Components) لموجة فولتية العاكس. الاستنتاجات النهائية قد تمت بمقارنة أداء المحرك باستخدام فولتية جيبيه وفولتية العاكس. لقد تم تطوير نموذج للدائرة المكافئة لإيجاد تيارات التوافقيات. أن تطوير هذا النموذج النظري تم باستخدام نتائج تحليل المجالات في الدوار الصلب. تيارات التوافقيات وتفاصيل أداء المحرك بما يشمل التداخلات المحتملة بين التوافقيات المتولدة سوية تم استنتاجها ومناقشتها. القراءات المقاسة لكل من التيار والعزم والقدرة على كل مدى السرعة ولكلا النوعين من التغذية، قد تم عرضها وقورنت مع النتائج والقيم النظرية. موجة التيار وموجة فولتية الطور والخط تم تحليلها مختبريا وقورنت مع النتائج النظرية. النتائج النظرية اتفقت بشكل جيد مع القيم العملية وتم تحديد التأثيرات الأكثر أهمية لهذه التوافقيات.

KEY WORDS
Harmonics, induction motor

INTRODUCTION

The most elementary type of rotor used in induction motors is the solid-steel rotor, which offers advantages in ease of manufacture, mechanically rigid and having good thermal properties. These features have made them attractive proposals to replace conventional rotors of induction motors, at least in some particular design and applications, and particularly for high-speed applications such as (20000-200000) rpm. The solid-rotor motor have high starting torque with low starting current, high rotor mass to absorb heat during repetitive starts, and a wide range of speed control for a narrow range of voltage variation. Many attempts have been made at improving their performance. Early attempts rely on using a soft-iron rotor with copper end plates [I. Woolley, 1973], to reduce the effective rotor resistance and achieve the desired torque. New attempts use different approaches of using composite rotor constructions [J. Saari, 1998, D. Gerling, 2000].

The development of static switching devices with high power ratings is leading to their continuously increasing application in the control of electrical machines. The static Inverters started replacing the old rotary converters. Inverters operation is based on the switching techniques. Therefore, their output is a nonsinusoidal voltage waveform. Fourier analysis show that inverter waveform contains many harmonics, when compared with old rotary converters. The solid-rotor motor has a significant advantage over conventional cage-rotor motors, when used in conjunction with solid-state drives [Leo A. Finzi, 1968]. Its rotor impedance have a numerical value which depends strongly on the magnitude of the voltage applied to the stator terminals for any given frequency [Leo A. Finzi, 1968]. The output voltage and current waveforms of the inverter are rich in harmonics, and these harmonics may have adverse effects on the motor performance. Harmonics can be a source of trouble in induction motors, producing extra losses and noise. The orders and magnitudes of the current harmonics which are present in the converter output depend on the design of the static converter and on the type of load, and are usually amenable to analysis by Fourier series.

The performance of induction motors operating on a nonsinusoidal voltage can be analyzed using different approaches. Among these are the equivalent circuit approach [G. C. Jain, 1964, B. J. Chalmers, 1968, A. M, 2001], the generalized machine theory approach and the multi-reference frame approach. The last two approaches yield time domain results making them convenient for analyzing the dynamic performance of induction motors [A. M, 2001]. Since the work presented in this paper deals with the steady-state performance, the equivalent circuit approach is adopted through out the presented work to comply with the Fourier analysis approach.

THEORY AND MODELING OF A SOLID-ROTOR INDUCTION MOTOR

A solid-rotor induction motor operates according to the same principles of operation as a conventional induction motor. The performance of such a motor is characterized by the nature of the interaction between the air-gap revolving field and the eddy currents induced in the solid-rotor, which develop the electromagnetic torque.

It is necessary to evaluate the impedance of the solid- rotor, both in phase and magnitude, to predict the behaviour of the motor under load conditions. The main difficulty in deriving an expression for this impedance arises from the extremely nonlinear magnetisation characteristic of the steel material. Many different approaches have been adopted to the calculation of eddy current loss in unlaminated magnetic materials aiming to develop an equivalent rotor impedance to be included in the parameters of motor equivalent circuit.

Early attempts are based on the assumption of material constant permeability, i.e. they considered the rotor as a linear medium. More realistic attempts used non-linear approximations to fit the magnetising curve, such as a limiting non-linear rectangular approximation. The limiting non-linear

method is well established and its result agrees well with practical measurements. It is simple to use, and widely-accepted since the magnetising force at the surface of the solid-rotor is usually high enough to drive the rotor material well into saturation. Both the non-linear and linear models has found application in the modeling of a solid-rotor machines.

SOLID-ROTOR MOTOR WITH SINE-WAVE SUPPLY

In the solid-rotor motor, the mechanism of flux penetration into the magnetic material depends greatly on the magnetic nonlinearity of the iron. Hence it is desirable to think in terms of equivalent circuit, it is recognized that the rotor circuit parameters have a peculiar property that for any given frequency, their numerical values depend strongly on the magnitude of the voltage applied to the stator terminals. To determine the rotor losses and torque of an induction machine with a solid-steel rotor, results of the approximate theory based on an rectangular B-H characteristic for steel material (which has been successfully used for a very wide range of applications which is called the limiting non-linear theory) is used in dealing with the fundamental voltage component as well as sine-wave supply.

The flux penetration into solid steel considers that the flux density within the steel may exist only at a magnitude equal to a saturation level $\pm B_s$. Thus for a given ϕ, as approximately occurs with a constant applied voltage, δ is constant and is independent on rotor frequency [B. J. Chalmers, 1984]. Using the limiting non-linear representation in the analysis of solid-rotor yield an expression for the equivalent rotor impedance referred to the stator [B. J. Chalmers, 1984, -1972- 1980-1982], the rotor phase angle is given by this analysis as 26.6°. Impedance expression is found upon analysis of the eddy-current losses at slip frequency in the solid rotor. The general form of the expression of rotor impedance is given in eq. (1)

$$Z_{2f}=\left(\frac{AmL^2N^2\rho B_s}{K_e D\phi s}\right)\angle\theta_2 \qquad (1)$$

Where

L: Rotor length

m : Number of stator phases.

N : Effective number of stator turn per phase.

ρ : Rotor resistivity.

B_s : Saturation flux density of the rotor material.

K_e : End effect factor [1].

D : Rotor diameter.

s: Slip

A and the phase angle θ_2 are constants.

The value of A is $(\frac{1280}{9\pi^3})$ and θ_2 is 26.6°. In practice the empirical adjustment of θ_2 to 30°, slightly above the value of 26.6°, gives consistently good correlation with practical results for a wide range of design [B. J. Chalmers, 1984, A. M. Saleh, 1985]. The variable quantities in eq. (1) are the slip s and the flux per pole ϕ, which is dependent on the air-gap voltage and this, in turn, varies with stator current owing to the presence of series stator impedance [B. J. Chalmers, 1972]. It is seen that Z_{2f} is inversely proportional to the product of flux and slip and this arises from the effect of the magnetic non-linearity of the rotor material. For an induction machine with uniform

air-gap flux the rotor impedance at the fundamental supply frequency can be expressed in terms of the air-gap voltage, E, [A. M. Saleh, 1985] as below

$$Z_{2f}=\left(\frac{AmL^2N^3\rho B_s f}{K_e DEs}\right)\angle\theta_2 \qquad (2)$$

Equivalent Circuit

The equivalent circuit of the polyphase induction motor with a solid-rotor, resulting from the treatment mentioned above, is shown in **Fig.(1)**, where r_1 and x_1 represent the stator winding resistance and leakage reactance, x_m represent the magnetizng reactance and Z_{2f} is the rotor equivalent impedance referred to the stator at the fundamental supply frequency eq. (2), the core losses is neglected. So far the circuit appears to have the same configuration as the familiar equivalent circuit of conventional polyphase induction motors.
The equivalent impedance per phase is given by

$$Z=Z_1+Z_m Z_{2f}/(Z_m+Z_{2f}) \qquad (3)$$

Where $Z_1=r_1+jx_1$,
$Z_m=jx_m$

The input power to the rotor per phase is given by

$$P_2=I_2^2 R_{2f} \qquad (4)$$

Where R_{2f} is the rotor resistance referred to stator (i.e. is the real part of Z_{2f}).
The rotor loss is ($s P_2$), then the developed gross output power per phase is

$$P=(1-s) P_2 \qquad (5)$$

The developed total torque is

$$T_1=3P/w_r \qquad (6)$$

But, $w_r=(1-s) w_s$, then

$$T_1=3P_2 / w_s = 3I_2^2 R_{2f} / w_s \qquad (7)$$

Where w_s is the synchronous speed of the stator field in rad/sec.

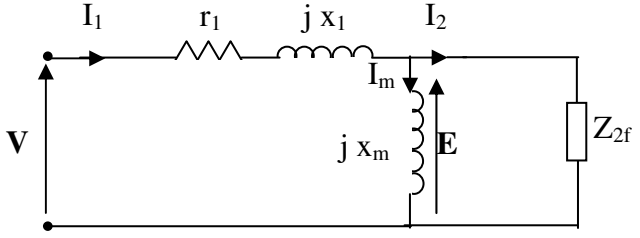

Fig. 1 Equivalent Circuit Per Phase

HARMONIC ANALYSIS OF 3-PHASE INVERTER

The application of symmetrical, nonsinusoidal three-phase voltages of constant periodicity to the motor terminals results in symmetrical nonsinusoidal three-phase motor currents. These currents may be thought to consist of a fundamental component plus higher time harmonics [Muhammad H. , 1993].

The waveform of inverter voltage depends upon the type of converter and the period of conduction of thyristors. It is rectangular or stepped waveform for 180° thyristor conduction angle. For a pulse width modulated inverter, output voltage waveform is a pulsed wave depending upon the method of modulation. The nonsinusoidal input wave is resolved into Fourier series. The behaviour of the machine is obtained by superposing the effects of fundamental and harmonics. This method provides informations about individual harmonic behaviour which reflect a guide to the inverter design.

Fourier Steady-State Analysis

The output voltage waveform of a three-phase inverter feeding a three-phase induction motor depends on the conduction period of the switching elements. The output waveform of the inverter is, however, periodic and can be analyzed using Fourier series. For symmetrical waveforms (the positive half cycle is the same as the negative half cycle) there will be no even order harmonics (i.e. 2,4,6,..etc.). Hence, by using Fourier series and according to the waveform shown in Appendix [A], the only orders of harmonics that can be affect machine performance are

$$n=6k \pm 1 \quad (8)$$

Where k=1,2,3,…etc.

According to the Appendix [A], the expression for the phase voltage, first phase, say v_a can be written as

$$v_a= \sum_{n=1,5,7,..}^{\infty} V_n \sin (nwt) \quad (9)$$

Where the constant V_n is determined as shown in appendix [A] depending on the shape of the waveform under consideration.

The harmonic of order n=6k-1 (such as n=5,11,17,…etc.) travels in a direction opposite to that of the fundamental field with the same number of poles as the fundamental field, i.e., it rotates at a speed equal to ((6k-1) N_s) [6]. The harmonics of order n=6k+1 (such as n=7,13,19,…etc.) travels in the same direction as the fundamental at a speed equal to ((6k+1) N_s).

The eq. (8) can be written in a more convenient form to indicate the sequence of the harmonic, too, as:

$$n=1 \pm 6k \quad (10)$$

Thus, the harmonic orders are -5,7,-11,13,…etc. The negative sign associated with the n^{th} harmonic represents a negative sequence harmonic order. Third harmonic voltages are in time phase, they form a zero-sequence voltages. They can not push a current in a star-connected stator windings with no neutral connection. All harmonics of order triple n will be zero-sequence, and therefore their effect will be negligible.

A time harmonic of order "n" results in a harmonic synchronous speed nN_s and if the machine is rotating at a speed N_r the n^{th} harmonic slip is given by

$$s_n= (nN_s \pm N_r) / nN_s \quad (11)$$

The negative sign in eq. (11) refers to forward rotating fields, obtained with harmonic order 1,7,13,…etc., while the positive sign refers to backward rotating fields, obtained with harmonic order 5,11,17,…etc. In terms of fundamental frequency slip, the time harmonic slip is found to be

$s_n=(n \pm (1-s))/ n$ (12)

Hence the frequency of the n^{th} harmonic rotor current is
$f_{2n}=s_n (nf_1)=[n-(1-s)] f_1$ (13)

For normal operation of an induction machine, s is usually very small and s is much less than n-1 and therefore
$s_n=(n-1) / n$ (14)
and,
$f_{2n} =(n-1) f_1$ (15)
Assuming that the saturation effect is negligible, that may arise due to superimposing voltages of different frequencies [1988], the principle of superposition can be applied to determine the overall performance of the 3-phase induction motor. Superposition principle rely on the assumption of linear systems. Therefore, this method is subject to the limitation imposed by the superposition principle. However, for nonsinusoidal voltage waveform, the motor behaviour for the fundamental is, as well as for individual harmonics are, determined independently and the net performance is assumed to be the sum of the contributions of each harmonic of the voltage waveform. The equivalent circuit of the induction motor is used in the analysis and the behaviour of the motor for each harmonic voltage is obtained by modifying the equivalent circuit for the harmonic under consideration. Thus a series of independent equivalent circuits (one for each harmonic) are used to calculate the complete steady state behaviour of the motor. The lack in the superposition principles is overcome by considering the possible interaction between field components which are present in the machine.

INVERTER FED SOLID-ROTOR MOTOR

An alternating magnetic field induces eddy currents in the material of iron cores. The eddy currents oppose the change of the flux, thus the magnetic field and flux can only penetrate to a certain depth within the magnetic material. The inner part of the material is left without flux. The depth of flux penetration is defined as the distance from a surface of a conductive material plane where an amplitude of an electromagnetic incident wave penetrating into the magnetic material [J. Lahteenmaki, 2002]. As the harmonic flux penetration into the rotor material is relatively small, the rotor is therefore assumed to have a constant permeability equal to the computed value at the rotor surface, and the surface impedance may be evaluated for each harmonic [D. O'Kelly, 1976]. The small harmonic flux component (of high frequency) is considered superimposed upon the larger fundamental component of flux. Results of the linear electromagnetic representation of the B-H curve is used in the analysis of a solid-rotor motor with nonsinusoidal supply. This method yields the classical depth of penetration which is dependent upon rotor angular frequency. The linear representation of the B-H characteristic of rotor steel, obviously, assumes a constant permeability, μ (i.e., B= μ H).

The assumption of linear magnetic material is non-realistic and this analysis is rarely used. However, it is widely used to treat cases of superimposed flux components rotating at different frequencies [B. J. Chalmers, A. M. Saleh, 1980-1982-1985]. The rotor impedance referred to the stator according to this method of analysis may be presented for each harmonic order under consideration as given below

$$Z_{2n} = \left(\frac{4\sqrt{2}mN^2L}{\sqrt{\pi}DK_e} \right) \left(\frac{\mu_\circ \mu_r \rho f_n}{s_n} \right)^{1/2} \angle 45^\circ \quad (16)$$

Where $f_n = nf_1$,

and,

$s_n = n \pm (1-s)/n$

This expression with a value of a phase angle of 45° and with a value of constant incremental permeability μ_r of 43 is used in the analysis of this study. Reference [10] gave a table with values of μ_r for different sizes of machines and ranges of electromotive forces, derived from tests carried out on rotor materials. The use of a constant value of μ_r of 43 was found acceptable during the experimental test over a wide range of positive and negative sequence field intensities [B. J. Chalmers, 1984, A.M. Saleh, 1985].

Harmonic Equivalent Circuit

The fundamental frequency equivalent circuit shown in **Fig. (1)** must be modified to take into account the harmonic frequencies. This can be achieved by introducing the following changes [B. J. Chalmers, 1977, A.M. Saleh, 2001]:

i- all reactances have a value of "n" times their value at the fundamental frequency f_1,

ii- the operating slip is the harmonic slip s_n.

The equivalent circuit of a solid-rotor induction motor with nonsinusoidal voltage supply appears to have the same configuration as the familiar equivalent circuit of a conventional induction motor under the same supply voltage as shown in **Fig. (2)**. The only difference is in the expression of the rotor impedance referred to the stator for harmonic orders under consideration as given in eq. (16) above.

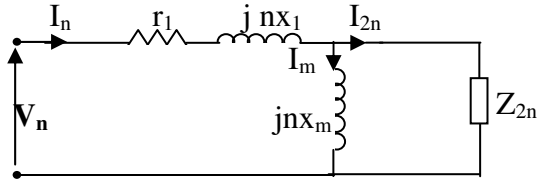

Fig. 2 Harmonic Equivalent Circuit Per Phase.

PRINCIPAL EFFECTS OF HARMONICS

The additional losses due to the presence of harmonic may be high if the supply waveform have large harmonic contents. These losses result from the increase in magnetic and ohmic losses. Magnetic losses are caused by harmonic main flux and harmonic leakage flux. Since rotor slip, s_n, is almost unity, stator harmonic current is reflected in the rotor and the resultant main harmonic flux is low. Magnetic loss in metallic parts caused by harmonic leakage flux is difficult to estimate [A.M. Saleh, 1985]. It is believed that ignoring these losses can introduce negligible error, due to the low level harmonic fluxes. Therefore the magnetic loss increase is considered negligible and loss increase is attributed, mainly, to the copper loss.

Stator Copper Losses

The total rms value of harmonic currents is given by

$$I_h = \sqrt{\sum_{n=5,7,..}^{\infty} I_n^{\,2}} \qquad (17)$$

Where I_h=harmonic currents.

The rms value of the total current is

$$I = \sqrt{I_1^{\,2} + I_h^{\,2}} \qquad (18)$$

The additional stator copper losses are determined by adding the losses due to each harmonic. Therefore, the increase in the stator copper losses is ($I_h^2 r_1$) and the total copper losses per phase can be written as [G. C. Jain, 1964, B. J. Chalmers, 1977]

$$P_s=I_1^2 r_1+I_h^2 r_1=I^2 r_1 \quad (19)$$

The above equation describes the loss increase if the supply waveform have large harmonic contents. The additional losses owing to time-harmonic currents will increase the conductor heating due to higher current flow. In large machines and due to the skin effect the resistance of windings is subject to further increase, too. Higher the frequency, higher the resistance, so when harmonic current flows, the resistance associated with a given harmonic will get increased amplifying the copper loses and increasing the heating of the machine. This is not considered in the present work.

Rotor Losses

For a conventional cage-rotor induction motor, the rotor resistance variation due to skin effect must be taken into consideration and particularly for deep-bar rotor construction. The rotor loss for every harmonic can be determined. The losses due to each harmonic are added to get the total losses. Usually, these additional rotor losses form a large portion of additional losses in the induction motor operating on a nonsinusoidal voltage [B. J. Chalmers, 1977].

For a solid-rotor induction motor, the rotor resistance for each harmonic order can be determined and the losses due to each harmonic order are determined and added to get the total rotor losses as given by

$$P_r=I_2^2 s R_{2f} + \sum_{n=5,7,..}^{\infty} I_{2n}^2 s_n R_{2n} \quad (20)$$

Mean Developed Torque

Due to the nonsinusoidal air-gap flux and rotor current, a torque is developed for each harmonic component as happens with the fundamental component. The developed torques can act in the forward or in the backward direction depending on the harmonic order [Subrahmanyam, Vedam., 1988].

A unidirectional harmonic torque is generated by the interaction between an air-gap flux and a rotor current component of the same harmonic frequency. It is noted that the net effect of torque harmonics is usually too small in comparison to motor rated torque [W. Shepherd, 1998], as will be explained hereunder.

Each harmonic produces an air-gap power and this power corresponds to a harmonic torque T_n acting at a speed of nw_s (radians per second). Thus, the air-gap power per phase is

$$T_n nw_s=I_{2n}^2 R_{2n} \quad (21)$$

Where R_{2n} is the resistance of a solid-rotor referred to stator at the frequency of the harmonic under consideration.

This torque can be positive or negative depending on the order of the harmonic under consideration. The equivalent torque in synchronous watts per phase, referred to the fundamental frequency is given by

$$T_n= I_{2n}^2 R_{2n} /n \quad (22)$$

For forward rotating fields of order 1,7,13,….etc., the torque is positive and for reverse rotating fields of order 5,11,17,….etc., the torque is negative. The net developed torque due to fundamental and harmonic currents are

$$T=T_1 \pm \sum_{n=5,7,....}^{\infty} T_n \qquad (23)$$

Where T_1 is the fundamental torque.
The positive sign refers to the torque of a harmonic order in the same direction of fundamental torque (i.e., n=7,13,19,…) and the negative sign refers to the torque of a harmonic order in the reverse direction of fundamental torque (i.e., n=5,11,17,…). Although, the net harmonic torques are acting against the fundamental one, it is clear that T_n is very small and the most significant torque reduction arises from the low order harmonics (i.e., 5^{th} and 7^{th}).

Torque Pulsation

The fundamental useful steady state torque is developed by the interaction between the fundamental stator air-gap flux and the rotor current. This is a steady constant torque i.e., it does not pulsate in magnitude. However, it is superimposed by the parasitic torques which may be either steady or pulsating torques. Steady torques are due to interaction of air-gap flux and rotor current belonging to the same harmonic. As explained in the previous section, a fifth order harmonic produce braking torque as their direction of rotation is opposite to that of the fundamental. A seventh order harmonic produce a motoring torque as their rotation is in the forward direction. In addition to the unidirectional harmonic torques, a pulsating torque is developed due to interaction between air-gap flux and rotor current belonging to different harmonics.

This pulsating torque whose frequency is the difference between the frequencies under consideration [A. M. Saleh, 2001]. For example, the pulsating torque pulsating at $6f_1$ is generated when fundamental flux reacts with either fifth or seventh harmonic rotor currents. The result is a torque pulsation of six times the fundamental frequency superimposed on the steady-state unidirectional torque [W. Shepherd, 1998].

Table (1) summarises the possible interaction of harmonics with each other and the frequency or the direction of the resulting torque. The interaction can be denoted by flux (or magnetizing current) and rotor current [A. M. Saleh, 2001]. All harmonics co-exist and the following torques, up to the seventh harmonic, are generated by the interactions between their fluxes and currents: -

a)I_m I_2 : the fundamental torque.
b)I_{m5} I_{25} and I_{m7} I_{27} : the torque of each harmonic current.
c)I_m I_{25} and I_m I_{27} : torque of harmonic currents and fundamental flux.
d)I_{m5} I_2 and I_{m7} I_2 : torque of fundamental current and harmonic fluxes.
e)I_{m5} I_{27} and I_{m7} I_{25} : torque of harmonic currents and fluxes.

The torques in (a) and (b) are steady torque and non-pulsating and have been covered in previous sections. Since I_{m5} and I_{m7} are very small, and the most significant pulsation of torque is resulting from the interaction between fundamental flux and harmonics currents, that in (c) above, and the torque in (d) and (e) are of negligible importance. For the fundamental component, the air-gap power is equal to the developed mechanical power which can be expressed as torque in (Newton-meters) acting at the synchronous speed. Thus, the torque per phase is given by

$$T_1 = E_1 I_2 \cos\Phi / w_s \qquad (24)$$

Where Φ is the phase angle between the air-gap voltage E_1 and rotor current I_2 and with solid-rotor its value is 30°, and $w_s=2\pi f_1/p=w_1/p$ where p is the number of pole pairs, then $w_s=w_1/p$.
E_1 is given by

$E_1=jI_mx_m=jI_mL_mw_1$ (25)

Where I_m is the magnetizing current and L_m is the magnetizing inductance.
From the phasor diagram shown in **Fig. (3)**, $\theta = 60^\circ$ and one can show that ($I_2 \cos\Phi = I_2 \sin\theta$), therefore,

$T_1=0.866p\ I_mL_mI_2$ (26)

Fig. (4) shows the phasor diagram of a harmonic, and from this phasor diagram the harmonic torque per phase is given by

$T_n=pI_{mn}\ L_mI_{2n} \cos\Phi_n= pI_{mn}\ L_mI_{2n} \sin\theta_n$ (27)

Where $\Phi_n=\theta_n=45^\circ$. Therefore,

$T_n=0.707pI_{mn}\ L_mI_{2n}$ (28)

From the combined phasor diagram shown in **Fig. (5)** the varying torque is

$T_v=I_mL_mp\ (I_{25} \sin(\theta_5-45^\circ) +I_{27} \sin(\theta_7+45^\circ))$ (29)

with $\theta_5=\alpha-6wt$

$\theta_7=\gamma+6wt$

Where α and γ are the values of θ_5 and θ_7 at wt=0. For any square symmetrical waveform $\alpha=\gamma=0$ or π [7]. Thus,

$T_v=I_mL_mp\ (I_{27} \sin(6wt+45^\circ) -I_{25} \sin(6wt+45^\circ))$ (30)

Since $I_mL_m=E_1/w_1$, then,

$T_v=(E_1/w_1)p(I_{27} – I_{25}) \sin(6wt+45^\circ)$ (31)

For a conventional induction motor, the torque pulsation can be expressed as [A. M. Saleh, 2001]

$T_v=(E_1/w_1)p(I_{27} – I_{25}) \sin(6wt)$ (32)

This expression is the same as that in solid-rotor induction motor as given by eq. (31). The only difference from solid-rotor is the phase shift of (45°) in torque waveform. Therefore, this torque pulsate at six times the supply frequency. In the absence of 5^{th} and 7^{th} harmonics, the 11^{th} and 13^{th} harmonics give pulsation at twelve times the supply frequency. The motor torque pulsation can be made smaller by increasing the magnetizing inductance, and by reducing the direct-current ripple when the motor is on no-load [G. K. Creightion, 1980]. It might be possible to reduce the torque pulsations by lowering the ripple current with a high-frequency dc link chopper [G. K. Creightion, 1980].
The self-reactance of the induction motor have great influence on the amplitude of torque pulsation. An external reactance can be added to a low reactance machines to reduce the torque pulsation [A. M. Saleh, 2001]. However, this may effect the fundamental torque and it is applicable to small machine of low output torque. The main effect of torque pulsation result from the low order harmonic. Usually the lower pulsating frequency is much higher than the natural frequency of the

mechanical system composed of the rotor and the coupled load. The high inertia of the rotating part can damp out these oscillation at the shaft at normal running speeds. However, for wide range variable speed drives an analysis of the mechanical resonance speeds is necessary to avoid damages due to possible amplification of pulsating torque at resonance.

Table (1) Reaction of Stator and Rotor Harmonics

Stator Harmonic	Rotor Harmonic	Nature of Torque	Direction or Frequency of pulsation
1	1	Steady	Forward
1	5^{th}	Pulsating	$6f_1$
1	7^{th}	Pulsating	$6f_1$
1	11^{th}	Pulsating	$12f_1$
1	13^{th}	Pulsating	$12f_1$
5^{th}	1	Pulsating	$6f_1$
5^{th}	5^{th}	Steady	Backward
5^{th}	7^{th}	Pulsating	$12f_1$
5^{th}	11^{th}	Pulsating	$6f_1$
5^{th}	13^{th}	Pulsating	$18f_1$
7^{th}	1	Pulsating	$6f_1$
7^{th}	5^{th}	Pulsating	$12f_1$
7^{th}	7^{th}	Steady	Forward
7^{th}	11^{th}	Pulsating	$18f_1$
7^{th}	13^{th}	Pulsating	$6f_1$
11^{th}	1	Pulsating	$12f_1$
11^{th}	5^{th}	Pulsating	$6f_1$
11^{th}	7^{th}	Pulsating	$18f_1$
11^{th}	11^{th}	Steady	Backward
11^{th}	13^{th}	Pulsating	$24f_1$

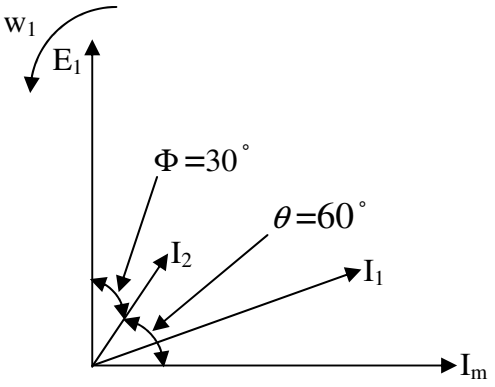

Fig. (3) Fundamental Phasor Diagram

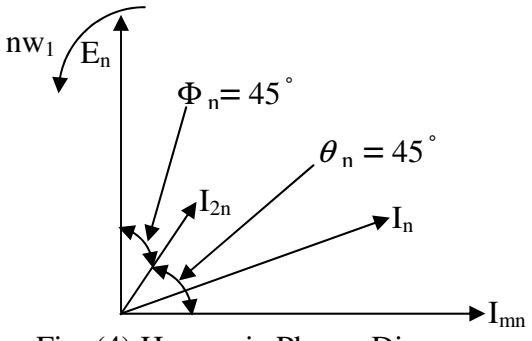

Fig. (4) Harmonic Phasor Diagram

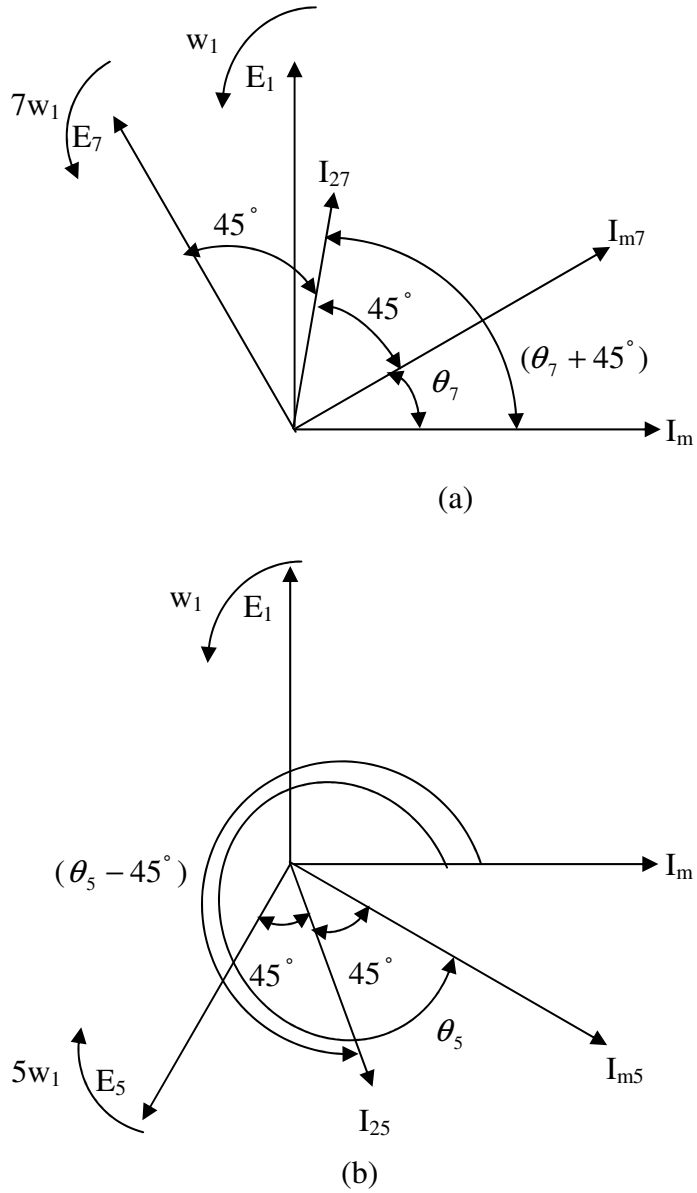

Fig. (5) Combined Phasor Diagram
(a) Fundamental and 7th harmonic
(b) Fundamental and 5th harmonic

SIMULATION AND EXPERIMENTAL RESULTS

The induction motor used in simulation and in the experimental tests has the following characteristics: a three-phase induction motor with a conventional stator wounded with a four-pole three-phase windings. Fitted with a solid-steel rotor. The parameters of this motor were identified through the necessary tests. The parameters are given with operating motor data in appendix [B].
The three-phase induction motor was studied under nominal load for two different source conditions: i) sinusoidal and balanced three-phase supply. ii) Variable frequency inverter at 50Hz. The motor performance was calculated by computer simulation and found experimentally in the laboratory for the two conditions.

The three-phase motor with solid-rotor was tested with a sinusoidal supply at rated voltage and frequency. The calculated and measured stator input current as a function of slip is shown in **Fig. (6)**. It is clear that the calculated and experimental results are in a close agreement.
Torque/slip curve is given in **Fig. (7)** for the motor tested in the motoring condition. Experimental points are also shown in this figure. The measured torque, at a given slip, is in general less than the corresponding calculated values by not more than 4.1%. This is caused by neglecting the friction, windage (i.e. the mechanical losses) and surface losses in the simulation analysis.
The input power / slip curve is shown in **Fig. (8)**. This figure shows that the measured points at small values of slip are higher than the calculated points by an average error percent of 3.87%. This is owing to ignorance of the stator core losses in the simulation program and might be due to an error in wattmeter readings. **Fig. (9)** and **Fig. (10)** show oscillograms of phase and line voltage waveform of laboratory inverter with its wave analyzer result. This laboratory inverter is used to drive the solid-rotor motor in laboratory work with a square wave supply voltage at 50Hz whose fundamental voltage component equal to rated sinusoidal value.

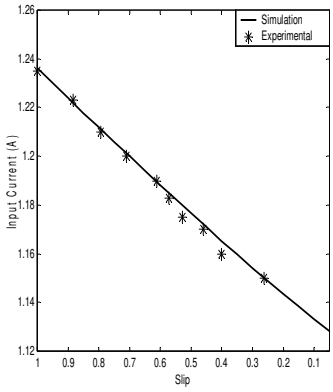

Fig. (6) Input Current versus Slip

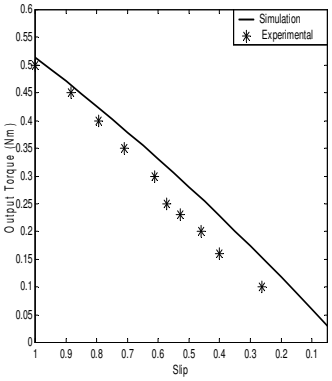

Fig. (7) Output Torque versus Slip

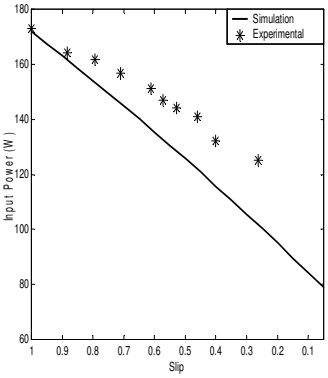

Fig. (8) Input Power versus Slip

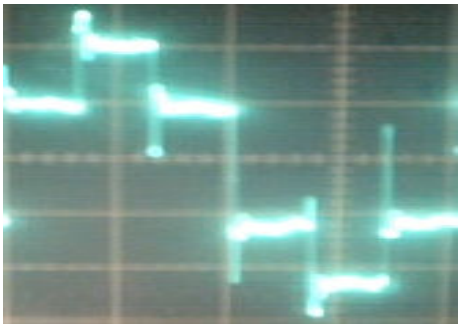

(a)

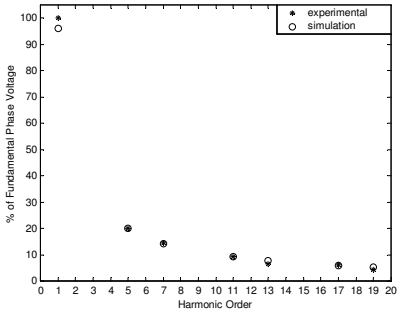

(b)

Fig. (9) Inverter phase voltage a) Experimental Waveform (50 v/div, 5ms/div) b) Results of Wave analyzer

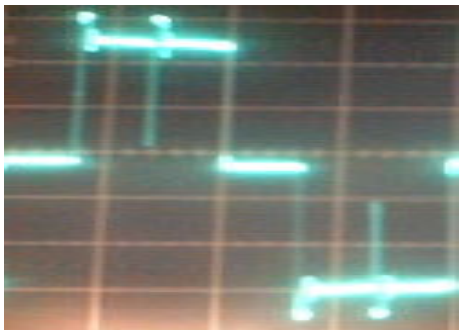

(a)

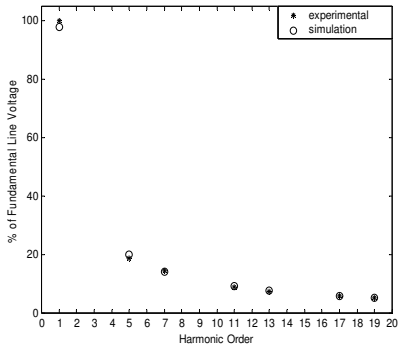

(b)

Fig. (10) Inverter line voltage
a) Experimental Waveform (50 v/div, 5ms/div)
b) Results of Wave analyzer

Fig. (11) show the simulation and measured stator input current as a function of slip of a solid-rotor motor fed by inverter. The Figure shows that the results are in good agreement. Torque /slip and input power curves are given in **Fig. (12)** and **Fig. (13)** respectively. The experimental torque measurement are lower than the calculated points by not more than 6.36%. This is caused by neglecting the friction, windage (i.e. the mechanical losses) and surface losses in the simulation analysis. The input power measured points are slightly greater than the calculated points at low slips by an average percent of error of 3.6%. This is owing to ignorance of the stator core losses in the simulation program and might be due to an error in wattmeter readings.

The simulation and experimental graphs of phase current of a solid-rotor motor with its wave analyzer for light load slip value of 0.263 obtained from the experimental machine and at standstill slip value of 1 are presented respectively in **Fig. (14)** to **Fig. (15)**. In the case of computer simulated current the results in the simulation are obtained considering up to 25th harmonic order. **Table (2)** shows the simulation and experimental DF and THD of the phase current calculated and measured up to 19th harmonic order. It is seen that, the DF results are in good agreement, while THD experimental results differ slightly by 13.2% from the calculated results. It is seen that, the DF and THD results are seems to be the same for the three slip values given in the table.

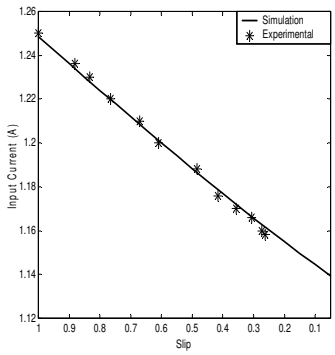

Fig. (11) Input Current versus Slip

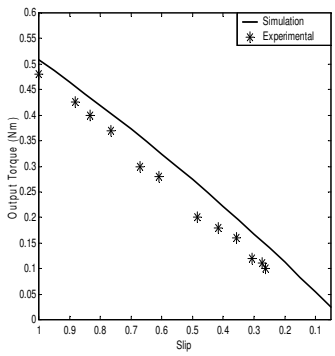

Fig. (12) Output Torque versus Slip

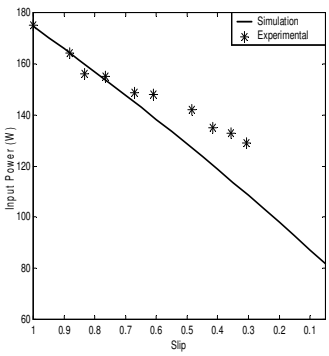

Fig. (13) Input Power versus Slip

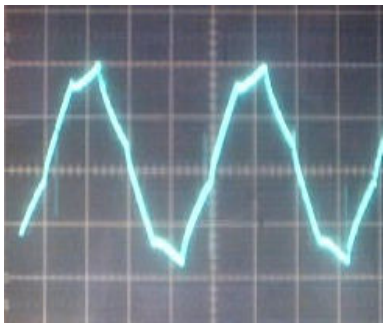

(a)

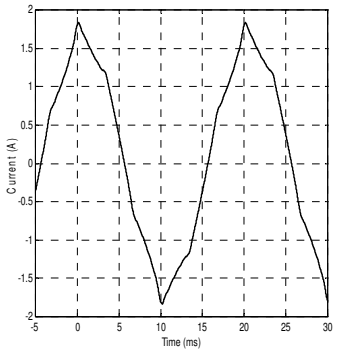

(b)

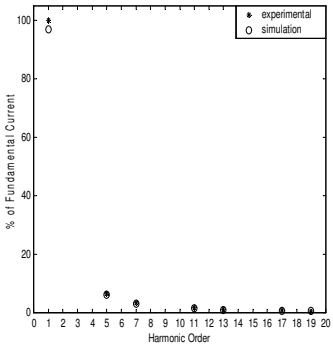

(c)

Fig. (14) Solid-Rotor Motor Phase Current at s=0.263
a) Experimental Waveform (1 A/div, 5ms/div)
b) Simulation Waveform
c) Results of Wave analyzer

(a)

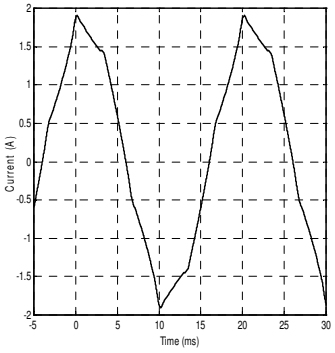

(b)

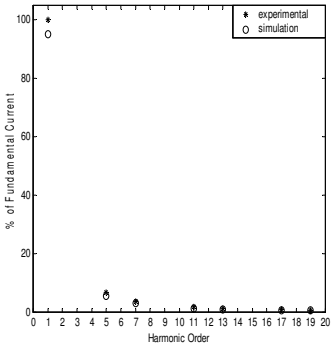

(c)

Fig. (15) Solid-Rotor Motor Phase Current at s=1
a) Experimental Waveform (2 A/div, 5ms/div)
b) Simulation Waveform
c) Results of Wave analyzer

Table (2) DF and THD of a Solid-Rotor Motor Current

Slip	Simulation		Experimental	
	DF(%)	THD(%)	DF(%)	THD(%)
0.263	99.7488	7.1	99.712	7.6
0.51	99.755	7.01	99.63	8.625
1	99.787	7	99.668	8.167

CONCLUSIONS

The most pronounce effect of harmonic voltages and currents on the induction motor is the increased heating due to the additional losses, mainly the copper losses associated with the harmonic currents. The increase in the input power of the motor due to the presence of harmonic is mainly consumed in the motor as losses forming an additional source of heat. The extra losses are dissipated within the stator and rotor of the machine. The loss increase due to presence of harmonics can consequently reduce the developed torque, due to temperature rise. The additional temperature rise increases stator and rotor resistance. Increases in these resistances reduce the fundamental torque of the machine. As a result, the overall efficiency of machine decreases as a consequence of the increase in losses. A solution to this problem could be the filtering of such harmonics at the inverter load. The steady harmonic torques are acting against each other and, at least for the machine under test, their net torque is small. The net harmonic torque is acting against the fundamental torque. The main effects of the harmonics on the operation of motors result from the low harmonics order. The harmonic content of the current depends upon the motor slip. It depends, to great extent, on the leakage reactance of the motor. A larger leakage reactance reduces the harmonic content of the current. The pulsating torques are produced by the interaction of the air-gap flux components (the fundamental flux and harmonic flux components) and rotor harmonic currents. The main torque pulsation result from the interaction between the low order rotor harmonic currents. The peak values of torque pulsation due to the low order harmonic frequency (i.e. 5^{th} and 7^{th}) is negligibly small for the motor under test. The pulsation reduces very greatly with increase of harmonic frequencies, since motor will have to withstand the pulsatio.. The calculated and measured results are in general in a close agreement for the two supplies conditions. The simulation and experimental DF results of a solid-rotor motor phase current are in good agreement. While, the THD experimental results differ by 13.2% from the calculated results. A solid-rotor motor has a lower input current than that of a conventional motor of the same frame size, when driven by inverter voltage supply. This is due to high rotor impedance of solid-rotor motor. Therefore, the stator losses are less than that in the case of conventional motor and the temperature rise of the motor is also less. As a result the efficiency of the solid-rotor motor is less sensitive than that of a cage-rotor motor with respect to supply type.

REFERENCES

I.Woolley and B.J. Chalmers; (1973), End Effects in Unlaminated-Rotor Induction Machines; Proc. IEE; vol.120; No.6; June.

J. Saari; (1998), Thermal Analysis of High-Speed Induction Machines; Dissertation for the degree of Doctor of Technology, Helsinki University, Finland;.

D. Gerling; (2000), Design an Induction Motor with Multilayer Rotor Structures and large gap; ICEM 2000, Finland; 28-30 August;; pp.458-461.

Leo A. Finzi and Derek A. Paice; (1968), Analysis of the Solid-Iron Rotor Induction Motor for Solid- State Speed Controls; IEEE Transaction on Power Apparatus and Systems; vol. PAS-87; No.2; February; p.590.

G.C. Jain; (1964), Effect of Voltage Waveshape on Performance of a 3-Phase Induction Motor; IEEE Trans.; PAS-83;; p.561.

B.J. Chalmers and B.R. Sarker; (1777), Induction Motor Losses due to Nonsinusoidal Supply Waveforms; Proc. IEE; vol.115; No.12; December 1968; p..

A.M. Saleh; (2001), Effects of Time Harmonics on Induction Gyromotors; IJCCCE; No.2; vol.2;; p.1.

B.J. Chalmers and A.M.Saleh; (1984), Analysis of Solid-Rotor Induction Machines; IEE Proc.; vol.131; No.1; pt.B; January.

B.J. Chalmers and I. Woolley; (1972), General Theory of Solid-Rotor Induction Machines; Proc. IEE; vol.119; No.9; September.

B.J. Chalmers and R.H. Abdel-Hamid; (1980), Parameters of Solid-Rotor Induction Machines with Unbalanced Supply; Proc. IEE; vol.127; No.3; Pt.B; May.

B.J. Chalmers; (1982), Application of Induction Machines with Solid-Steel Secondaries; Universities Power Engineering Conference UMIST Manchaster, England;.

B.J. Chalmers and A.M. Saleh; (1984), Single-Phase Capacitor-Run Induction Motors with Solid-Steel Rotor; Proceedings International Conferences on Electrical Machines, Lausanne Switzerland; pt.3; 18-21 September;.

A.M. Saleh; (1985), Analysis of Induction Machines with Unlaminated and Composite Secondaries; Ph.D. Thesis; University of Manchester;.

Muhammad H. Rashid; (1993), Power Elecronics; Prentice-Hall International, Inc,.

Subrahmanyam, Vedam; (1988), Thyristors Control of Electric Drives; Mc Graw-Hill: New Dellhi;.

J. Lahteenmaki; (2002), Design and Voltage Supply of High-Speed Induction Machines"; Dissertation for the degree of Doctor of Technology, Helsinki University, Finland;.

D.O'kelly; (1976), Theory and Performance of Solid-Rotor Induction and Hysteresis Machines; Proc. IEE; vol.123; No.5; May.

W.Shepherd and D.T.W. Liang; (1998), Power Electronics and Motor Control"; Cambridge University press,.

G.k. Creighton; (1980), Current-Source Inverter-fed Induction Motor Torque Pulsation; Proc. IEE; vol.127;pt.B; No.4; July.

Appendix [A]

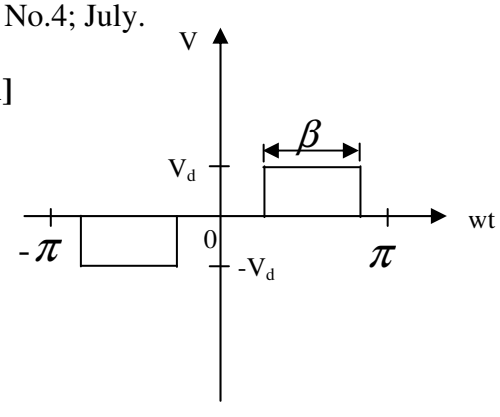

Fig. (A.1)

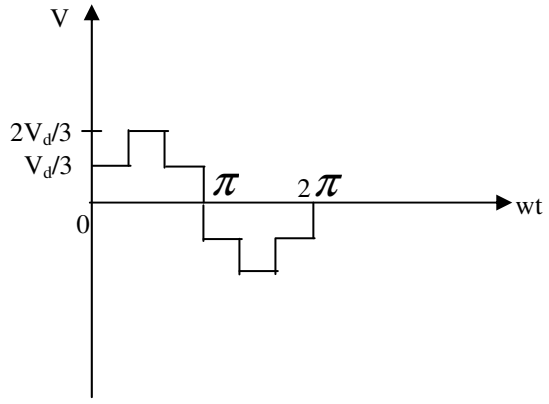

Fig. (A.2)

Consider the general form for square-wave shown in **Fig. (A.1)** where β represent conduction period.

$$v(wt)=\begin{cases} -V_d & -(\pi+\beta)/2<wt<-(\pi-\beta)/2 \\ 0 & -(\pi-\beta)/2<wt<(\pi-\beta)/2 \\ V_d & (\pi-\beta)/2<wt<(\pi+\beta)/2 \end{cases}$$

V(-wt)=-V(wt) therefore $b_n=0$, i.e., no cosine term.
The function have symmetry about the x-axis therefore $a_0=0$.
$v(wt+\pi)=-v(wt)$ therefore $a_{2n}=0$

$$a_n=2V_d/\pi \int_{(\pi-\beta)/2}^{(\pi+\beta)/2} \sin(nwt)\, dwt$$

$$=-2V_d/n\pi\,[\cos n((\pi+\beta)/2)-\cos n((\pi-\beta)/2)]$$

$$=4V_d/n\pi\,[\sin n\beta/2.\sin n\pi/2]$$

For $\beta=180^\circ$,

$$a_n=4V_d/n\pi\,[\sin n\pi/2]^2$$

and,

$$V=\sum_{n=1}^{\infty} 4V_d/n\pi \sin nwt$$

Let $4V_d/\pi=\sqrt{2}\,E_a$, then,

$$v=\sum_{n=1}^{\infty} \sqrt{2}\,E_a/n \sin nwt$$

Where E_a is the rms value of the fundamental component.
For $\beta=120^\circ$,

$$a_n=4V_d/n\pi\,[\sin n\pi/3]\,[\sin n\pi/2]$$

$$=2\sqrt{3}\,V_d/n\pi \sin m\,wt \quad | \ |$$

Where
$m=1\pm 6k$ for k=1,2,3,……,etc.
$n=m*(-1)^{(m+3)/2}$ | |
So if $\sqrt{2}\,E_a=2\sqrt{3}\,V_d/\pi$, it follows that

$$v=\sqrt{2}\,E_a[\sin(wt)-1/5\sin(5wt)-1/7\sin(7wt)+1/11\sin(11wt)+1/13\sin(13wt)+\ldots\ldots..]$$

Similarly, for the stepped-voltage waveform shown in **Fig. (A.2)**, which it is have the same properties of **Fig. (A.1)** and by applying Fourier analysis yields that: -

$$v=2V_d/\pi\,[\sin(wt)+1/5\sin(5wt)+1/7\sin(7wt)+1/11\sin(11wt)+1/13\sin(13wt)+\ldots\ldots..]$$

or

$$v=\sum_{n=1}^{\infty} 2V_d/n\pi \sin(nwt)$$

Appendix [B]

Motor name plate

FB ELECTRICAL MACHINE TUTOR / ENGLAND

Type: EMT-180
Number of Poles, p: 4
Number of Phases, m: 3
Connection: Δ / Y
Power, W: 250
Voltage, V: 138/240
Frequency, Hz: 50
Current, A: 2.5
Per-phase parameters at 50 Hz obtained by Test : -

Stator data

Element	Value
Stator resistance per phase, r_1, Ω	19
Stator reactance per phase, x_1, Ω	24
Stator magnetizing reactance per phase, x_m, Ω (with solid-rotor)	98
Effective number of stator winding turns in series per phase, N	780

For Solid-Rotor

The experimental machine under test, it is the same type and rating of the experimental machine used in the test in the work presented in reference [10]. Therefore, the values of rotor saturation flux density, B_s, and rotor resistivity, ρ, used in the analysis of this work are the same that used in the reference [10] as given below:

B_s 1.8 W_b/m^2

ρ 22e-8 Ω.m

Rotor length and diameter are measured directly in the lab as given below:

L 0.034 m
D 0.1m

The value of End-effect factor (K_e), for the experimental rotor without end-plates is obtained from reference [1] as given below:

K_e 0.185